Measurement of the optical properties of solid biomedical phantoms at the National Institute of Standards and Technology

Paul Lemaillet*[a], David W. Allen [a], Jeeseong Hwang [b]
[a]National Institute of Standards and Technology, 100 Bureau Drive, Gaithersburg, MD 20899
[b]National Institute of Standards and Technology, 325 Broadway Street, Boulder, CO 80305

ABSTRACT

Solid phantoms that serve as a proxy for human tissue provide a convenient test subject for optical medical imaging devices. In order to determine the quantitative performance of a given system, the absolute optical properties of the test subject must be known. Currently there is no national scale applicable to the scattering and absorption properties of solid diffuse tissue phantoms that would provide traceability and estimated measurement uncertainties for optical imaging applications. This paper describes progress in the development of a facility dedicated to the determination of the optical properties of solid biomedical phantoms. A brief description of the system, data analysis, Graphical User Interface (GUI), and measurement uncertainties is presented. The design is based on a double-integrating sphere, steady-state domain approach. The initial evaluation of the system includes the measurement of solid phantoms and a comparison to the manufacturer's values that were determined by a time resolved approach. The initial results indicate that measurement agreement is within the estimated uncertainties with the coverage factor k=2.

Keywords: solid biomedical phantoms, double-integrating spheres, adding doubling, uncertainty budget

1. INTRODUCTION

The biomedical community relies on phantoms mimicking the optical properties of tissues to develop, test and/or calibrate biomedical optical devices. These tissue simulating phantoms can be built using different types of scatterers (TiO_2/Al_2O_3 powder, Intralipid [1], calibrated polymer or glass microspheres), an absorber (ink, molecular dyes) and supporting materials (aqueous suspension, silicon, polyurethane resin) [2] [3] [4]. The chosen components are then mixed and sometimes cured (solid phantoms). Ultimately the optical properties of the resulting phantoms need to be measured. Many measurement technique are available (time of flight [5], multi-distance measurement of fluence, measurement of total reflectance and transmittance [3] [6], but the measurement results need to be compared to those obtained from a reference standard. A diffusive liquid reference standard using Intralipid as a scatterer with well-defined optical properties (absorption coefficient, μ_a; reduced scattering coefficient, μ_s') to be measured with an uncertainty smaller than 2 % has been proposed [7] [8] [9]. However, liquid phantoms are not practical for dissemination and solid phantoms are favored as reference standard. Bouchar et. al. [5] measured μ_a and μ_s' of solid tissue simulating phantoms manufactured by the Institut National d'Optique (Biomimic, INO Inc., Quebec, Canada) with respective uncertainties (coverage factor k=1) of about 6 % and 3.5 % using a time resolved transmittance measurement technique.

At this time, there is no National Institute of Standards and Technology (NIST)-traceable reference standard for calibration of biomedical optical devices and this paper presents NIST progress toward filling this gap. We measure the optical properties of commercially available INO biomedical phantoms with a double integrating sphere setup in the continuous wave (CW) domain [3] [10] [11]. Analysis of the data (total reflectance and total transmittance) is performed with an inversion procedure similar to Prahl's Inverse Adding Doubling [12]. Our procedure allows the computation of a complete uncertainty budget for each sample measurement. A Graphical User Interface (GUI) was developed to facilitate using the data analysis program is presented.

2. MATERIALS AND METHODS

2.1 Experimental setup

Figure 1 diagrams the experimental setup. The polarization of an incident HeNe laser beam (λ=543.5 nm, JDS Uniphase Corporation, Milpitas, CA, USA; λ=632.8 nm, Research Electro-Optics, Inc., Boulder, CO, USA) is controlled by a linear Glan-Taylor polarizer, P, which is followed by a beam splitter, BS. The light is at normal incidence to a sample, S, held

*paul.lemaillet@nist.gov

Design and Performance Validation of Phantoms Used in Conjunction with Optical Measurement of Tissue VII, edited by David W. Allen, Jean-Pierre Bouchard, Proc. of SPIE Vol. 9325, 932504 · © 2015 SPIE
CCC code: 1605-7422/15/$18 · doi: 10.1117/12.2085110

between two integrating spheres, R and T (UMBK-190, Gigahertz Optik, Türkenfeld, Germany; internal diameter: 196 mm; entrance port diameter: 25.1 mm; sample port diameter: 38.1 mm; detector port diameter: 12.7 mm; coated with ODM98 synthetic material). A reference signal is detected by photodiode D1 and the total reflectance signal and the total transmittance signal are measured by photodiode D2 and D3, respectively (D1, D2, D3; Edmunds Optics Inc., Barrington, NJ, USA). The photocurrent is amplified by three P-9202-6 amplifiers (Gigahertz optic) connected to a DAQ board (NI PCI-6110, National Instruments Corporation, Austin, TX, USA) and monitored by a Lab program for data acquisition. A 99 % reflectance standard, R_{Std}, blocks the exit port of the transmittance sphere during the measurements.

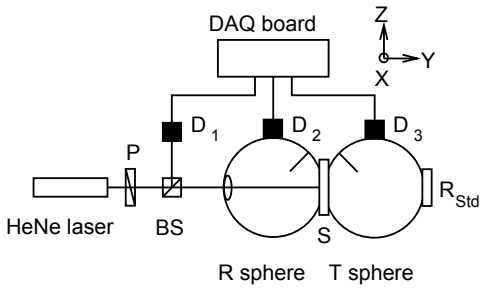

Figure 1. Experimental setup: P: polarizer; BS: beam splitter: D1, D2 and D3: photodiodes; S: sample; R_{Std}: reflectance standard; R and T spheres: reflectance and transmittance spheres.

2.2 Samples

The samples are manufactured by INO and are commercially available. In general, the samples consist of a supporting material, polyurethane, with titanium dioxide (TiO_2) as a scatterer and carbon black as an absorbing component. The samples are designed to match nominal values of the optical parameters ($\mu_a = 0.01\ \mathrm{mm}^{-1}$, $\mu_s' = 1\mathrm{mm}^{-1}$ at $\lambda = 805$ nm). The samples have a 100 mm square base and come in three different thicknesses, $d = 5.15$ mm, 7.11 mm and 9.85 mm. A custom made holder was used to hold the sample by opposite corners to minimize the contact area.

2.3 Measurements

The measurement procedure requires measuring the total reflectance and the total transmittance of the sample. The measured total reflectance is the ratio of the light intensity reflected from the sample to the light intensity reflected from a NIST certified nominal 99 % reflectance standard R_{Std}, successively set at the sample port of the reflectance sphere:

$$R_{\mathrm{Meas}} = R_{\mathrm{Std}} \frac{I_{\mathrm{Sample}}}{I_{\mathrm{Standard}}} \tag{1}$$

where I_{i} are the normalized intensities computed from the measured voltages for both the signal channel and the reference channel, $VR_{\mathrm{i}}^{\mathrm{Signal}}$ and $VR_{\mathrm{i}}^{\mathrm{Ref}}$; $I_{\mathrm{i}} = \frac{VR_{\mathrm{i}}^{\mathrm{Signal}} - VR_{\mathrm{Dark}}^{\mathrm{Signal}}}{VR_{\mathrm{i}}^{\mathrm{Ref}} - VR_{\mathrm{Dark}}^{\mathrm{Ref}}}$ with $\mathrm{i} = \mathrm{Sample}, \mathrm{Standard}$, $VR_{\mathrm{Dark}}^{\mathrm{Signal}}$ and $VR_{\mathrm{Dark}}^{\mathrm{Ref}}$ are the background measurement obtained while blocking the laser beam.

The measured total transmittance is the ratio of the light intensity transmitted with the sample in place to a transmission measurement with no sample:

$$T_{\mathrm{Meas}} = \frac{I_{\mathrm{Sample}}}{I_{\mathrm{Empty}}}, \tag{2}$$

where I_{i} are the normalized intensities computed from the measured voltages for both the signal channel and the reference channel, $VT_{\mathrm{i}}^{\mathrm{Signal}}$ and $VT_{\mathrm{i}}^{\mathrm{Ref}}$; $I_{\mathrm{i}} = \frac{VT_{\mathrm{i}}^{\mathrm{Signal}} - VT_{\mathrm{Dark}}^{\mathrm{Signal}}}{VT_{\mathrm{i}}^{\mathrm{Ref}} - VT_{\mathrm{Dark}}^{\mathrm{Ref}}}$ with $\mathrm{i} = \mathrm{Sample}, \mathrm{Empty}$, $VT_{\mathrm{Dark}}^{\mathrm{Signal}}$ and $VT_{\mathrm{Dark}}^{\mathrm{Ref}}$ are the background measurements.

The details on how to make these optical properties measurements can be found elsewhere [3] [12] [13].

2.4 Data analysis

The Adding-Doubling method was used with a home-made inversion routine to compute the optical properties of the samples. Adding-Doubling is valid for samples with homogeneous optical properties and infinite plane-parallel slab geometry. It first solves the Radiative Transfer Equation (RTE) for a thin layer in the single scattering approximation and computes the total reflectance and total transmittance by successively adding/doubling the values until the thickness of the sample is reached. The inversion routine solves for the optical properties of the sample using the measured total reflectance and transmittance. It is similar to the Inverse Adding Doubling procedure from Prahl [3] [6] but allows for some flexibility in the choice of the model for the integrating sphere. Using the Guide to the expression of Uncertainty in Measurement (GUM) [14], our method also enables the computation of the uncertainty budget for the measurements of the optical properties of the sample by considering the statistical uncertainty (type A uncertainty) on the measurements and the non-statistical uncertainty (type B uncertainty) on the samples parameters, on the integrating spheres parameters, on the detectors reflectance and on the calibration standards reflectance. A graphical user interface (GUI) was developed to facilitate the data analysis (Figure 2).

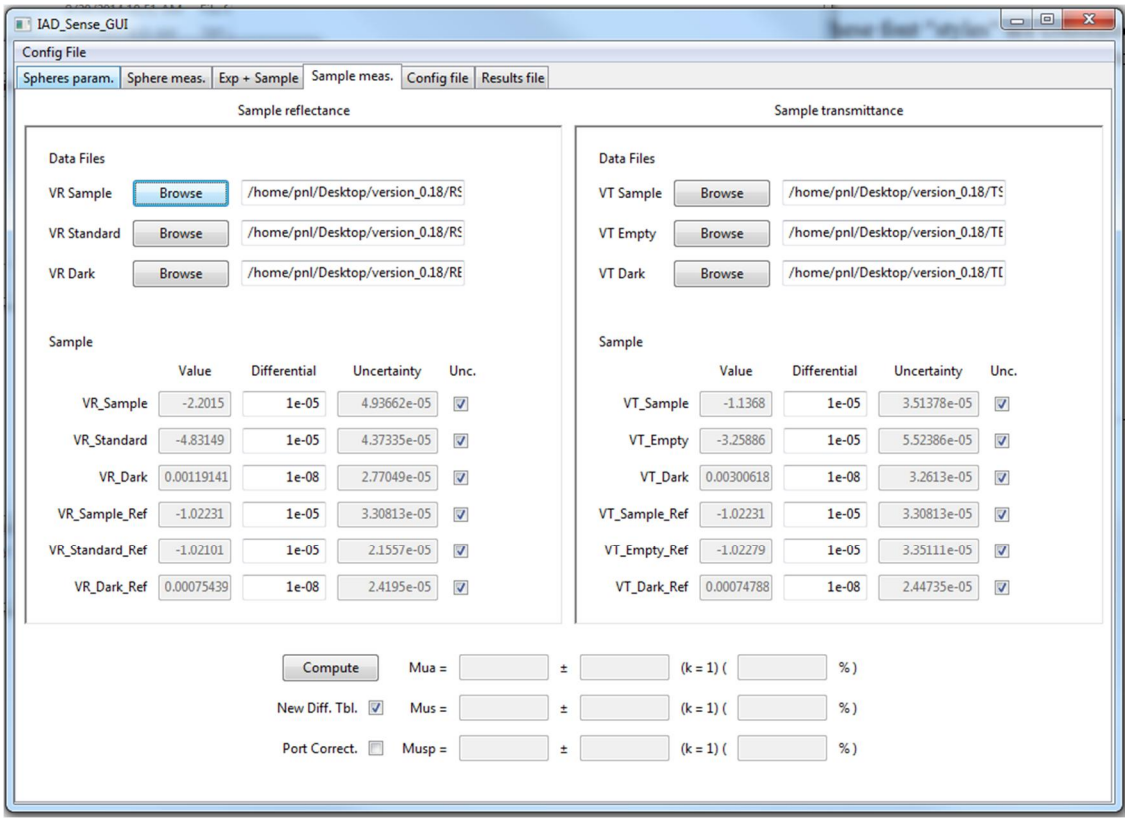

Figure 2. Graphical user interface: sample measurement and optical property computation tab.

3. RESULTS

Figure 3 and Figure 4 present the optical properties μ_a, and μ_s', measured respectively at λ=543.5 nm and λ=632.8 nm for three 100 mm-square INO phantoms of thicknesses $d = 5.15$ mm, 7.11 mm and 9.85 mm. The measured values are compared to the ones measured by INO at the same wavelengths. The uncertainty on the INO results were estimated from the measurements at $\lambda = 660$ nm [5]. The results in Figure 3 and Figure 4 are present the results with 1 x σ error bars (i.e. coverage factor $k = 1$). At λ=543.5 nm, our results are consistent with the values from INO for both μ_a and μ_s'. At λ=632.8 nm, our values of μ_s' are consistent with the one from INO at all sample thicknesses, but for μ_a, the agreement is only for $d = 9.85$ mm. However, with a coverage factor $k = 2$, preferred by NIST [15], the optical properties measured here agree with the results provided by INO. Table 1 summarizes the results and the uncertainty with $k = 2$ for our measurements and the ones measured by INO.

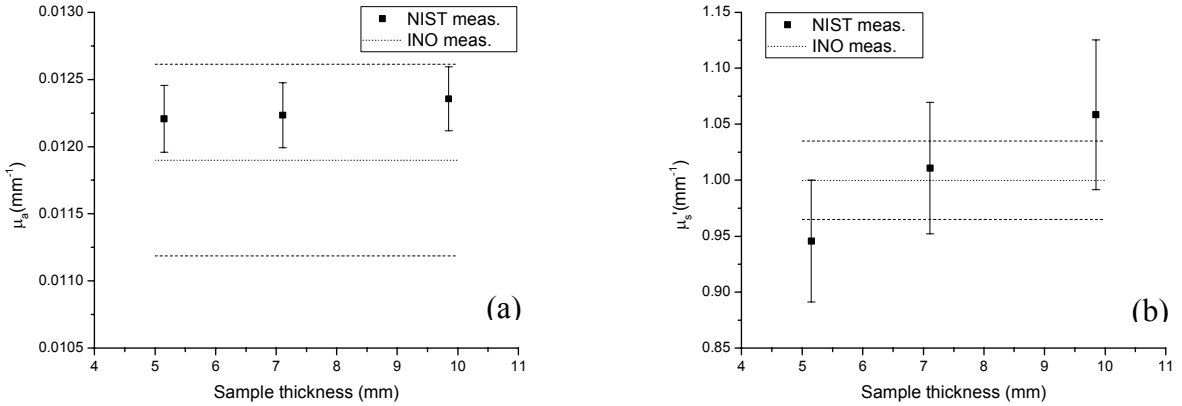

Figure 3. Results at λ=543.5 nm of: (a) μ_a, the absorption coefficient of the sample and (b) μ_s', the reduced scattering coefficient of the sample, versus the thickness for 100 mm-square INO phantoms. The error bars (coverage factor *k*=1) are obtained for each experiment by propagation of the type A and type B uncertainties The NIST results are compared to the values from INO (mean value and error, dotted lines).

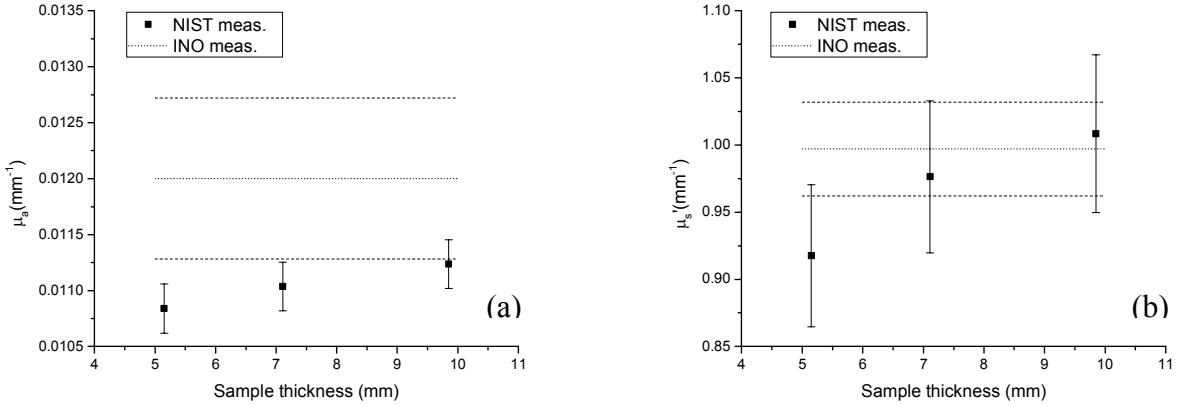

Figure 4. Results at λ=632.8 nm of: (a) μ_a, the absorption coefficient of the sample and (b) μ_s', the reduced scattering coefficient of the sample, versus the thickness for 100 mm-square INO phantoms. The error bars (coverage factor *k*=1) are obtained for each experiment by propagation of the type A and type B uncertainties. The NIST results are compared to the values from INO (mean value and error, dotted lines).

Table 1: Results and uncertainties ($k = 2$) of: μ_a, the absorption coefficient of the sample; μ_s', the reduced scattering coefficient the sample. The measurements are at $\lambda = 543.5$ nm and $\lambda = 632.8$ nm. The uncertainties on the INO results were estimated from measurements at $\lambda = 660.0$ nm [5].

	Thickness	Parameter	Value	Absolute uncertainty	Relative uncertainty
$\lambda = 543.5\ nm$					
	5.15 mm	μ_a	$0.0122\ \text{mm}^{-1}$	$4.96 \times 10^{-4}\ \text{mm}^{-}$	4.06%
		μ_s'	$0.946\ \text{mm}^{-1}$	$0.109\ \text{mm}^{-1}$	11.5 %
	7.11 mm	μ_a	$0.0122\ \text{mm}^{-1}$	4.84×10^{-4} mm	3.95%
		μ_s'	$1.01\ \text{mm}^{-1}$	$0.117\ \text{mm}^{-1}$	11.6 %
	9.85 mm	μ_a	$0.0124\ \text{mm}^{-1}$	4.77×10^{-4} mm	3.86 %
		μ_s'	$1.06\ \text{mm}^{-1}$	$0.123\ \text{mm}^{-1}$	11.6 %
INO		μ_a	$0.0119\ \text{mm}^{-1}$	$1.43 \times 10^{-3}\ \text{mm}^{-}$	12 %
		μ_s'	$1.0\ \text{mm}^{-1}$	$0.07\ \text{mm}^{-1}$	7 %
$\lambda = 632.8\ nm$					
	5.15 mm	μ_a	$0.0108\ \text{mm}^{-1}$	$4.41 \times 10^{-4}\ \text{mm}^{-}$	4.07 %
		μ_s'	$0.918\ \text{mm}^{-1}$	$0.106\ \text{mm}^{-1}$	11.5 %
	7.11 mm	μ_a	$0.0110\ \text{mm}^{-1}$	$4.36 \times 10^{-4}\ \text{mm}^{-}$	3.95 %
		μ_s'	$0.976\ \text{mm}^{-1}$	$0.113\ \text{mm}^{-1}$	11.6 %
	9.85 mm	μ_a	$0.0112\ \text{mm}^{-1}$	$4.33 \times 10^{-4}\ \text{mm}^{-}$	3.85 %
		μ_s'	$1.01\ \text{mm}^{-1}$	$0.117\ \text{mm}^{-1}$	11.7 %
INO		μ_a	$0.012\ \text{mm}^{-1}$	$1.44 \times 10^{-3}\ \text{mm}^{-}$	12 %
		μ_s'	$0.997\ \text{mm}^{-1}$	$0.0698\ \text{mm}^{-1}$	7 %

4. CONCLUSION

In this paper, we presented measurements of the optical properties of solid biomedical phantoms at $\lambda = 543.5$ nm and $\lambda = 632.8$ nm and compared the results to the values obtained from their manufacturer, INO. The samples were measured using our double-integrating sphere setup in the steady state domain. The measured data consist of the total transmittance and the total reflectance of the sample, and analysis of the data was based on a home-made inversion routine of the Adding-Doubling procedure, which solves the radiative transfer equation (RTE) iteratively for the data. Our inversion routine computed the optical parameters and the uncertainty budget for each measurement. A GUI was developed to facilitate the data analysis. The samples were three square solid phantoms of thicknesses $d = 5.15$ mm, 7.11 mm and 9.85 mm. There is an agreement between our results and the ones from INO. The uncertainty on the optical parameters measured were about 4.0 % for μ_a and 11.5 % for μ_s', compared to 12 % and 7 %, respectively obtained by INO [5]. Future work in developing this facility will include extending the capabilities to cover a broad spectral range, analyzing liquid samples, and implementing an in depth analysis of the associated uncertainties. Inter-laboratory comparisons with other national metrology institutes will be investigated.

5. ACKNOWLEDGMENT

This work was supported by the NIST Innovative Measurement Science (IMS) program on “optical medical imaging for clinical applications” and NIST intramural research program in Statistical Engineering Division of the Information Technology Laboratory of NIST. Drs. Jessica Ramella-Roman and Steven Jacques for useful suggestions.

REFERENCES

[1] *Certain commercial materials and equipment are identified in order to adequately specify the experimental procedure. Such identification does not imply recommendation by the National Institute of Standards and Technology.*.

[2] B. W. Pogue and M. S. Patterson, "Review of tissue simulating phantoms for optical spectroscopy, imaging and dosimetry," *Journal of Biomedical Optics,* vol. 11, no. 4, pp. 041102-041102-16, 2006.

[3] T. Moffitt, Y.-C. Chen and S. A. Prahl, "Preparation and characterization of polyurethane optical phantoms," *Journal of Biomedical Optics,* vol. 11, no. 4, pp. 041103-041103-10, 2006.

[4] M. L. Vernon, J. Fr\'{e}chette, Y. Painchaud, S. Caron and P. Beaudry, "Fabrication and characterization of a solid polyurethane phantom for optical imaging through scattering media," *Appl. Opt.,* vol. 38, no. 19, pp. 4247-4251, Jul 1999.

[5] J.-P. Bouchard, I. Veilleux, R. Jedidi, I. Noiseux, M. Fortin and O. Mermut, "Reference optical phantoms for diffuse optical spectroscopy. Part 1- Error analysis of a time resolved transmittance characterization method," *Opt. Express,* vol. 18, no. 11, pp. 11495-11507, May 2010.

[6] S. A. Prahl, M. J. C. van Gemert and A. J. Welch, "Determining the optical properties of turbid media by using the adding--doubling method," *Appl. Opt.,* vol. 32, no. 4, pp. 559-568, Feb 1993.

[7] P. Di Ninni, F. Martelli and G. Zaccanti, "Intralipid: towards a diffusive reference standard for optical tissue phantoms," *Physics in Medicine and Biology,* vol. 56, no. 2, p. N21, 2011.

[8] F. Martelli and G. Zaccanti, "Calibration of scattering and absorption properties of a liquid diffusive medium at NIR wavelengths. CW method," *Opt. Express,* vol. 15, no. 2, pp. 486-500, Jan 2007.

[9] L. Spinelli, F. Martelli, A. Farina, A. Pifferi, A. Torricelli, R. Cubeddu and G. Zaccanti, "Calibration of scattering and absorption properties of a liquid diffusive medium at NIR wavelengths. Time-resolved method," *Opt. Express,* vol. 15, no. 11, pp. 6589-6604, May 2007.

[10] C. Böcklin, D. Baumann, F. Stuker, J. Klohs, M. Rudin and J. Fröhlich, "Reconstructing optical parameters from double-integrating-sphere measurements using a genetic algorithm," *Proc. SPIE,* vol. 8583, pp. 858304-858304-8, 2013.

[11] V. T. J. Keränen and A. J. Mäkynen, "Double integrating sphere system for optical parameter determination of industrial suspensions," *Proc. SPIE,* vol. 7022, pp. 70220T-70220T-8, 2007.

[12] S. A. Prahl, *http://omlc.ogi.edu/software/iad/.*

[13] T. P. Moffitt, "Light Transport in Polymers for Optical Sensing and Photopolymerization," 2005.

[14] I. O. for Standardization, Guide to the expression of uncertainty in measurement (GUM)-Supplement 1: Numerical methods for the propagation of distributions, vol. ISO draft guide DGUIDE99998, Geneva: International Organization for Standardization, 2004.

[15] B. N. Taylor, C. Ntnoef, B. N. Taylor, C. E. Kuyatt and R. H. Brown, "Guidelines for evaluating and expressing the uncertainty of NIST measurement results," 1994.